Poincaré's velocity representation in time domain free surface flow

Choi Y.-M.[1], Malenica Š.[2], Clément, A.H.[1], Bouscasse B.[1], and Ferrant P.[1]

[1] *Ecole Centrale de Nantes, Nantes, France CNRS UMR 6598*

[2] *Bureau Veritas, Paris, France*

Introduction

The efforts to couple viscous and inviscid flows in naval and offshore engineering have been studied from the early 90s. The researches showed a possibility of reducing the computational domain but the most of researches are concluded to the increase of total computation cost and complexity of methodology [2, 3]. Because two-way coupling needs to solve two different flows, it makes the methodology complex and unfavorable. One-way coupling which blends or subtracts the wave components in the computation domain and/or equations are attempted by many researchers [6, 7, 9]. But two-way coupling is not carefully studied. Noblesse [8] presented a new potential flow representation. The velocity in a potential flow region can be computed explicitely from the velocity distribution on the boundary surfaces. He suggested a generic representation and applied it for the case of steady flow, time-harmonic and time-harmonic with forward speed flows. Guillerm and Alessandrini [4] showed the result of two-way coupling between velocity representation and viscous flow for the steady forward speed case. As the velocity representation are presented only for the case of steady and time-harmonic cases, the present study introduces a velocity representation in time-domain free surface flow.

Formulation

The boundary integral equation states that the velocity potential at the field point is given by boundary integral equation(BIE). The velocity in potential flow region is expressed by applying a gradient on BIE as,

$$\nabla_x \Phi(\mathbf{x}) = \nabla_x \psi - \nabla_x \chi, \tag{1}$$

where

$$\nabla_x \psi = \oiint_S \{\mathbf{n}_\xi \cdot \nabla_\xi \Phi(\boldsymbol{\xi})\} \nabla_x G(\mathbf{x};\boldsymbol{\xi}) dS, \qquad \nabla_x \chi = \oiint_S \Phi(\boldsymbol{\xi}) \nabla_x \{\mathbf{n}_\xi \cdot \nabla_\xi G(\mathbf{x};\boldsymbol{\xi})\} dS \tag{2}$$

where Φ is the velocity potential, $\mathbf{x} = (x, y, z)$ and $\boldsymbol{\xi} = (\xi, \eta, \zeta)$ are the field and source points, respectively. $\mathbf{n}_\xi$ is a normal vector to the boundary surface S and it points inside of fluids domain. ∇_ξ and ∇_x are the spatial derivatives with respect to the source and field point coordinates. Noblesse [8] showed that the dipole induced velocity is identical with,

$$\nabla_x \chi = \left[u^d, v^d, \pm w^d\right]^T = \oiint_S \{\Phi(\boldsymbol{\xi}) \times \mathbf{n}_\xi\} \times \nabla_x G(\mathbf{x};\boldsymbol{\xi}) dS \tag{3}$$

where Green function has the following relationship:

$$\left(\frac{\partial}{\partial x}, \frac{\partial}{\partial y}, \frac{\partial}{\partial z}\right) G(\mathbf{x}, \boldsymbol{\xi}) = \left(-\frac{\partial}{\partial \xi}, -\frac{\partial}{\partial \eta}, \mp \frac{\partial}{\partial \zeta}\right) G(\mathbf{x}, \boldsymbol{\xi}).$$

The contribution of dipole is replaced with the vortex at boundary surface with the first derivatives of Green function. It states that the velocity at field point is given explicitely if the velocity distribution on the boundary is known. This equation is called as Poincaré's velocity representation. The wave Green function for infinite depth is expressed with the combination of source, image source and wave terms as

$$4\pi G^{\pm} = \begin{cases} -\dfrac{1}{r} \pm \dfrac{1}{r'} \pm H \\ -\dfrac{1}{r} \mp \dfrac{1}{r'} \pm F \end{cases}, \tag{4}$$

where r and r' is the source and image source. H and F are the wave or harmonic terms. By changing the sign of image source, the source and its image satisfy the homogeneous Dirichlet and Neumann conditions on the mean free surface. Using the equation (4), the integral over mean free surface is given as:

$$\iint_{S_F} \begin{bmatrix} \Phi_n G_\xi^+ + (\nabla_\xi \Phi \times \mathbf{n}_\xi)^\zeta G_\eta^+ - (\nabla_\xi \Phi \times \mathbf{n}_\xi)^\eta G_\zeta^+ \\ \Phi_n G_\eta^+ + (\nabla_\xi \Phi \times \mathbf{n}_\xi)^\xi G_\zeta^+ - (\nabla_\xi \Phi \times \mathbf{n}_\xi)^\zeta G_\xi^+ \\ \Phi_n G_\zeta^- + (\nabla_\xi \Phi \times \mathbf{n}_\xi)^\eta G_\xi^- - (\nabla_\xi \Phi \times \mathbf{n}_\xi)^\xi G_\eta^- \end{bmatrix} dS = -\iint_{S_F} \begin{bmatrix} \Phi_\zeta H_\xi + F_\zeta \Phi_\xi \\ \Phi_\zeta H_\eta + F_\zeta \Phi_\eta \\ \Phi_\xi F_\xi + \Phi_\eta F_\eta - \Phi_\zeta H_\zeta \end{bmatrix} dS. \tag{5}$$

Noblesse [8] suggested this integral as a generic expression for the free surface flow. The time domain Green function of infinite water depth is given as,

$$\begin{aligned} 4\pi G(\mathbf{x}, \boldsymbol{\xi}; t) &= -\frac{1}{r} + \frac{1}{r'} - 2\int_0^\infty dk \left\{1 - \cos\left(\sqrt{gk}t\right)\right\} e^{kZ} J_0(kR) \\ &= -\frac{1}{r} - \frac{1}{r'} + 2\int_0^\infty dk \cos\left\{\sqrt{gk}t\right\} e^{kZ} J_0(kR), \end{aligned} \tag{6}$$

where $Z = z + \zeta$, $R = \sqrt{(x-\xi)^2 + (y-\eta)^2}$. Therefore it satisfies the generic expression. To obtain the total velocity representation in time domain, the boundary surfaces are splitted into the matching-wake surface (S_{MW}), the free surface (S_F) and the surface at infinity distance (S_∞). The time derivatives of velocity from equation (3) is given as

$$\begin{bmatrix} u_\tau \\ v_\tau \\ w_\tau \end{bmatrix} = -\iint_{S_{MW} \cup S_F \cup S_\infty} \begin{bmatrix} \Phi_{n\tau} G_\xi^+ + (\nabla_\xi \Phi_\tau \times \mathbf{n}_\xi)^\zeta G_\eta^+ - (\nabla_\xi \Phi_\tau \times \mathbf{n}_\xi)^\eta G_\zeta^+ \\ \Phi_{n\tau} G_\eta^+ + (\nabla_\xi \Phi_\tau \times \mathbf{n}_\xi)^\xi G_\zeta^+ - (\nabla_\xi \Phi_\tau \times \mathbf{n}_\xi)^\zeta G_\xi^+ \\ \Phi_{n\tau} G_\zeta^- + (\nabla_\xi \Phi_\tau \times \mathbf{n}_\xi)^\eta G_\xi^- - (\nabla_\xi \Phi_\tau \times \mathbf{n}_\xi)^\xi G_\eta^- \end{bmatrix} dS, \tag{7}$$

It is assumed that the boundary surface do not change with time. By applying the integral by parts in time and the radiation condition on equation (7), the total velocity at time t is expressed as

$$\begin{aligned} \mathbf{u}(\mathbf{x}, t) = &-\iint_{S_{MW} \cup S_F} \left\{\Phi_n(\boldsymbol{\xi}, t) \nabla_\xi \mathcal{G}(\mathbf{x}, \boldsymbol{\xi}, 0) + \nabla_\xi \mathcal{G}(\mathbf{x}, \boldsymbol{\xi}, 0) \times (\nabla_\xi \Phi(\boldsymbol{\xi}, t) \times \mathbf{n}_\xi)\right\} dS \\ &+ \int_{t_0}^t d\tau \iint_{S_{MW} \cup S_F} \left\{\Phi_n(\boldsymbol{\xi}, \tau) \nabla_\xi \mathcal{G}_\tau(\mathbf{x}, \boldsymbol{\xi}, t-\tau) + \nabla_\xi \mathcal{G}_\tau(\mathbf{x}, \boldsymbol{\xi}, t-\tau) \times (\nabla_\xi \Phi(\boldsymbol{\xi}, \tau) \times \mathbf{n}_\xi)\right\} dS, \end{aligned} \tag{8}$$

where

$$\mathcal{G} = \begin{cases} G^+ & x\text{-},y\text{-directional velocity components, e.g. } (u, v) \\ G^- & z\text{-directional velocity component e.g. } (w) \end{cases} . \tag{9}$$

The velocity potential and time domain Green function satisfy the following relationships on the mean free surface,

$$\Phi_{\tau\tau} + g\Phi_\zeta = 0, \qquad \text{and} \qquad H_{\tau\tau} + gF_\zeta = 0 \qquad \text{on} \qquad \zeta = 0. \tag{10}$$

Substituting the free surface boundary condition and applying Stokes and Reynolds transport theorems on equation (8), the total velocity in time domain free surface flow is obtained as equation (11). The total velocity has four components: the rankine source ($\mathbf{u}_R$), the image source ($\mathbf{u}_{R^*}$), the harmonic term ($\mathbf{u}_H$) and the free surface ($\mathbf{u}_F$).

$$4\pi \mathbf{u}(\mathbf{x}, \boldsymbol{\xi}, t) = \mathbf{u}_R + \mathbf{u}_{R^*} + \mathbf{u}_H + \mathbf{u}_F \tag{11}$$

where

$$\mathbf{u}_R\left(\mathbf{x},\boldsymbol{\xi},t\right) = -\iint_{S_{MW}} \left\{\Phi_n(\boldsymbol{\xi},t)\nabla_\xi \mathcal{R}(\mathbf{x},\boldsymbol{\xi}) + \nabla_\xi \mathcal{R}(\mathbf{x},\boldsymbol{\xi}) \times (\nabla_\xi \Phi(\boldsymbol{\xi},t) \times \mathbf{n}_\xi)\right\} dS \tag{12}$$

$$\hat{\mathbf{u}}_{R^*}\left(\mathbf{x},\boldsymbol{\xi},t\right) = -\iint_{S_{MW}} \left\{\Phi_n(\boldsymbol{\xi},t)\nabla_\xi \mathcal{R}'(\mathbf{x},\boldsymbol{\xi}) + \nabla_\xi \mathcal{R}'(\mathbf{x},\boldsymbol{\xi}) \times (\nabla_\xi \Phi(\boldsymbol{\xi},t) \times \mathbf{n}_\xi)\right\} dS \tag{13}$$

$$\hat{\mathbf{u}}_H\left(\mathbf{x},\boldsymbol{\xi},t\right) = \int_{t_0}^{t} d\tau \iint_{S_{MW}} \left\{\Phi_n(\boldsymbol{\xi},\tau)\nabla_\xi H_\tau(\mathbf{x},\boldsymbol{\xi},t-\tau) + \nabla_\xi H_\tau(\mathbf{x},\boldsymbol{\xi},t-\tau) \times (\nabla_\xi \Phi(\boldsymbol{\xi},\tau) \times \mathbf{n}_\xi)\right\} dS \tag{14}$$

$$\begin{aligned}\hat{\mathbf{u}}_F(\mathbf{x},t) = &-\int_{t_0}^{t} d\tau \int_{C_{MW}} \nabla_\xi F(\mathbf{x},\boldsymbol{\xi},t-\tau) \times \left\{\nabla_\xi \Phi\left(\boldsymbol{\xi},\tau\right) \times \mathbf{k}\right\} U_n^{2D} dl \\ &- g\int_{t_0}^{t} d\tau \int_{C_{MW}} \left\{\nabla_\xi F(\mathbf{x},\boldsymbol{\xi},t-\tau) \times \mathbf{t}\right\} \mathit{\Xi}(\boldsymbol{\xi},\tau) dl + \int_{t_0}^{t} d\tau \int_{C_{MW}} \nabla_\xi H_\tau(\mathbf{x},\boldsymbol{\xi},t-\tau) \mathit{\Xi}(\boldsymbol{\xi},\tau) U_n^{2D} dl\end{aligned} \tag{15}$$

where ˆ represents the sign of vertical component is opposite. $\mathcal{R} = -1/r$ and $\mathcal{R}' = 1/r'$. C_{MW} is a cross-sectioned waterline of matching and mean free surfaces. $\mathbf{t}$ is a tangential vector. $\mathit{\Xi}$ is the wave elevation. U_n^{2D} is the transport velocity. Above velocity representation only have the flow properties in the right-hand side, e.g., velocity, wave elevation and transport velocity at boundary surface. Therefore, the velocity can be computed by explicitely without solving the equations if flow properties on the matching surface are given.

Results and Discussion

Hulme's heaving hemisphere is selected as a benchmark test to validate the velocity representation [5]. The heaving hemisphere locates inside of the arbitrary matching-wake surface(S_{MW}) and it oscillates with constant amplitude and frequency(ω). The velocity, wave elevation and transport velocity on the matching-wake surface is given to reconstruct the velocity at field point. The computed velocity from Poincaré representation is compared with analytic solution. The various matching-wake surfaces which are shown in figure 1 are considered for the validation.

The computed velocities using Poincaré representation are compared in figure 2. When the field point locates relatively far from the free surface ($z = -1$), the reconstructed velocity from Poincaré representation shows a good agreement with analytic solution. But the reconstructed velocity becomes unstable as the field point closes to the free surface ($z \approx 0$). The line integral along the waterline gives a poor numerical results because Green function has a diverging behavior when the source and field points together locates on the free surface. It is known as the singular behavior of *waterline integral* in time domain problem [1]. The reconstructed velocities on the free surface are shown in figure 3 with increasing the number of sub-line segment. The reconstructed velocities are seen to be better as the number of sub-line segment increases. It is expected to have a good result when the special care is applied to the waterline integral.

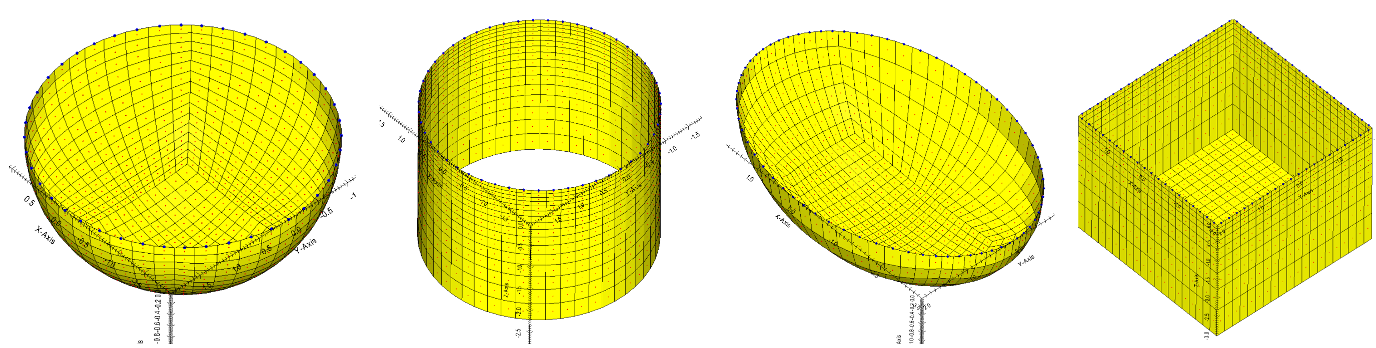

(a) Hemisphere (b) Cylinder shell (c) Semi-ellipsoid (d) Parallel pipe

Figure 1: Various matching-wake surface (S_{MW}), the heaving hemisphere locates inside of surface.

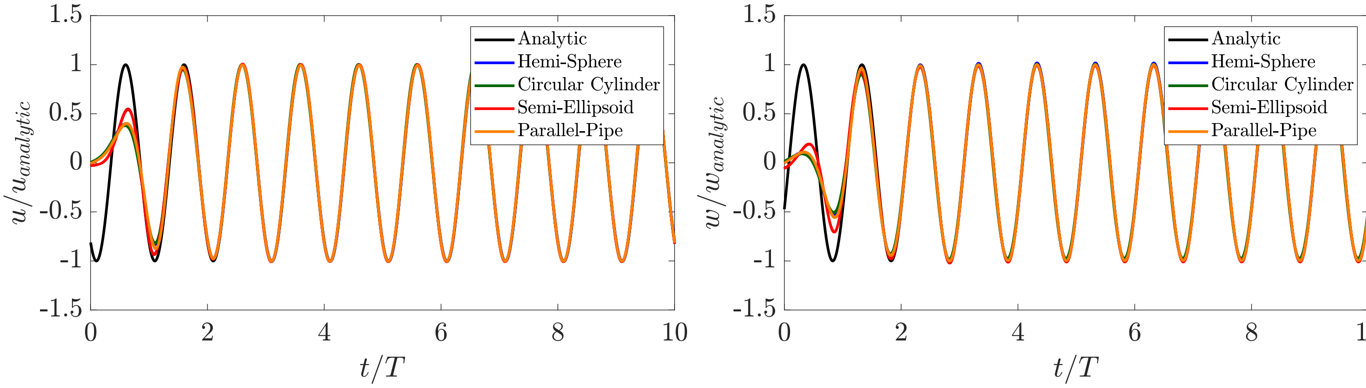

Figure 2: Reconstructed velocity from Poincaré representation with various matching-wake surfaces (S_{MW}), $\mathbf{x} = (5, 0 - 1)$.

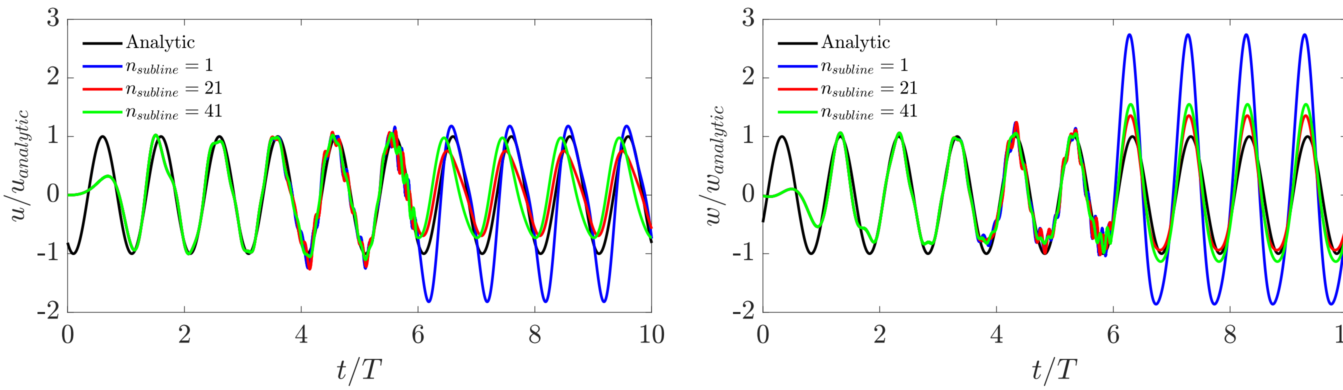

Figure 3: Reconstructed velocity on the free surface with increasing the number of sub-line segment, $\mathbf{x} = (5, 0, 0)$.

References

[1] Bingham, H. B. (1994). *Simulating ship motions in the time domain.* PhD thesis, Massachusetts Institute of Technology.

[2] Campana, E., Di Mascio, A., Esposito, P. G., and Lalli, F. (1995). Viscous-inviscid coupling in free surface ship flows. *Int. J. for Numerical Methods in Fluids*, 21(9):699–722.

[3] Chen, H. C., Lin, W. M., and Weems, K. M. (1993). Interactive zonal approach for ship flow including viscous nonlinear and wave effects. *6th Int. C. on Numerical Ship Hydrodynamics.*

[4] Guillerm, P.-E. and Alessandrini, B. (2003). 3D free-surface flow computation using a RANSE/Fourier-Kochin coupling. *International Journal for Numerical Methods in Fluids*, 43(3):301–318.

[5] Hulme, A. (1982). The wave forces acting on a floating hemisphere undergoing forced periodic oscillations. *Journal of Fluid Mechanics*, 121:443–463.

[6] Kim, J., Jaiman, R., Cosgrove, S., and O'Sullivan, J. (2011). Numerical wave trank analysis of wave run-up on a truncated vertical cylinder. *30th Int. C. on Ocean, Offshore and Arctic Engineering, OMAE2011-50283.*

[7] Li, Z., Bouscasse, B., Gentaz, L., Ducrozet, G., and Ferrant, P. (2018). Progress in coupling potential wave models and two-phase solvers with the SWENSE methodology. *37th Int. C. on Ocean, Offshore and Arctic Engineering, OMAE2018-77466.*

[8] Noblesse, F. (2001). Velocity representation of free-surface flows and Fourier-Kochin representation of waves. *Applied Ocean Research*, 23(1):41–52.

[9] Vukčević, V. (2016). *Numerical modelling of coupled potential and viscous flow for marine applications.* PhD thesis, University of Zagreb.